Current Genetics (2020) 66:345–359
https://doi.org/10.1007/s00294-019-01025-2

ORIGINAL ARTICLE

VdOGDH is involved in energy metabolism and required for virulence of *Verticillium dahliae*

Xiaokang Li[1,2] · Xiaofeng Su[2] · Guoqing Lu[2] · Guoqing Sun[2] · Zhuo Zhang[3] · Huiming Guo[2] · Ning Guo[1] · Hongmei Cheng[2]

Received: 16 April 2019 / Revised: 28 July 2019 / Accepted: 8 August 2019 / Published online: 17 August 2019

Abstract

Verticillium dahliae, a soil-borne fungus, can invade plant vascular tissue and cause *Verticillium* wilt. The enzyme α-oxoglutarate dehydrogenase (OGDH), catalyzing the oxidation of α-oxoglutarate in the tricarboxylic acid cycle (TCA), is vital for energy metabolism in the fungi. Here, we identified the *OGDH* gene in *V. dahliae* (*VdOGDH*, VDAG_10018) and investigated its function in virulence by generating gene deletion mutants (*ΔVdOGDH*) and complementary mutants (*ΔVdOGDH-C*). When the *ΔVdOGDH* mutants were supplemented with different carbon sources, vegetative growth on Czapek Dox medium was significantly impaired, suggesting that *VdOGDH* is crucial for vegetative growth and carbon utilization. Conidia of the *ΔVdOGDH* mutants were atypically rounded or spherical, and hyphae were irregularly branched and lacked typical whorled branches. Mutants *ΔVdOGDH-1* and *ΔVdOGDH-2* were highly sensitive to H_2O_2 in the medium plates and had higher intracellular ROS levels. *ΔVdOGDH* mutants also had elevated expression of oxidative response-related genes, indicating that *VdOGDH* is involved in response to oxidative stress. In addition, the disruption of *VdOGDH* caused a significant increase in the expression of energy metabolism-related genes *VdICL*, *VdICDH*, *VdMDH*, and *VdPDH* and melanin-related genes *Vayg1*, *VdSCD*, *VdLAC*, *VT4HR*, and *VaflM* in the *ΔVdOGDH* mutants; thus, *VdOGDH* is also important for energy metabolism and melanin accumulation. Cotton plants inoculated with *ΔVdOGDH* mutants exhibited mild leaf chlorosis and the disease index was lower compared with wild type and *ΔVdOGDH-C* strains. These results together show that *VdOGDH* involved in energy metabolism of *V. dahliae*, is also essential for full virulence by regulating multiple fungal developmental factors.

Keywords *Verticillium dahliae* · α-Oxoglutarate dehydrogenase · Energy metabolism · Pathogenicity

Introduction

The soil-borne filamentous fungus *Verticillium dahliae* Kleb. causes *Verticillium* wilt of cotton, one of the most destructive diseases of cotton worldwide. The disease is difficult to control because the hyphae of *V. dahliae* spread inside the xylem tissues, where they cannot be reached by fungicides (Klosterman et al. 2009). Melanized microsclerotia, long-lived dormant structures produced by *V. dahliae*, play a critical role in the disease cycle (Fradin and Thomma 2006; Klosterman et al. 2009). Microsclerotia germinate and produce several hyphae under the induction of plant root secretion (Pegg and Brady 2002). Numerous hyphae wrap around the root, but only a few hyphae adhere tightly to the root surface through the hyphopodium (Fradin and Thomma 2006; Klimes et al. 2015). As the infection structure of *V. dahliae*, the hyphopodium further differentiates and forms

Communicated by M. Kupiec.

Electronic supplementary material The online version of this article (https://doi.org/10.1007/s00294-019-01025-2) contains supplementary material, which is available to authorized users.

Xiaokang Li and Xiaofeng Su contributed equally to this work.

✉ Ning Guo
guoning@ahau.edu.cn

✉ Hongmei Cheng
chenghongmei@caas.cn

[1] School of Life Science, Anhui Agricultural University, Hefei 230036, China

[2] Biotechnology Research Institute, Chinese Academy of Agricultural Sciences, Beijing 100081, China

[3] Hunan Plant Protection Institute, Hunan Academy of Agricultural Sciences, Changsha 410125, China

a penetration peg to invade host plant cells and colonize the vascular tissue (Zhao et al. 2016). The extensive hyphal colonization can interfere with water transport within the vascular bundles (Vallad and Subbarao 2008), and lead to foliar chlorosis, necrosis, vascular discoloration, severe wilt, plant stunting, and even death (Fradin and Thomma 2006; Pegg and Brady 2002). Until now, the molecular determinants of the pathogenic mechanisms of *V. dahliae* have remained obscure; thus, identifying and analyzing the function of the genes involved in the pathogenic molecular mechanism have been critically needed.

Genomic sequencing and comparison of *V. dahliae* with *V. albo-atrum* has promoted the understanding of niche adaptation of plant vascular wilt pathogens and provided a valuable resource for further research (Klosterman et al. 2011). Several genes relevant to the virulence and pathogenic molecular mechanisms of *V. dahliae* have been identified (Klimes and Dobinson 2006; Rauyaree et al. 2005; Tzima et al. 2010; Zhang et al. 2019; Zhao et al. 2016). *Verticillium* transcription activator of adhesion Vta2 regulates fungal growth and conidiation, and host plant root invasion and H_2O_2 degradation, which is a major regulator of fungal pathogenesis (Tran et al. 2014). Tetraspanin (VdPls1) is known to recruit and activate membrane-bound NADPH oxidase (*VdNoxB*), a primary producer of reactive oxygen species (ROS). VdPls1/VdNoxB-mediated ROS production induces calcineurin-responsive zinc finger transcription factor Crz1 (VdCrz1) signaling, which is essential for penetration peg formation (Xiong et al. 2015; Zhao et al. 2016). Compared with the genomes of *V. dahliae* strains JR2 and VdLs.17, the genome of strain Vd991 (a defoliating isolate from cotton) has several exclusive lineage-specific regions 2 (G-LSR2), which was suggested to have been horizontally transferred from *Fusarium* (Chen et al. 2018a). Homology analysis indicates that the protein encoded by gene *VdDf7* within G-LSR2 may regulate the biosynthesis of *N*-lauroylethanolamine, which is critical for the defoliating phenotype (Zhang et al. 2019).

The initial disease process of phytopathogenic fungi can be divided into germination, proliferation, and penetration (Divon and Fluhr 2007; Solomon et al. 2003). The ability of phytopathogenic fungi to penetrate plants and utilize the available nutrient sources is critical for successful invasion. For fungal metabolism, lipolysis provides energy for conidia germination and penetration and glycolysis is critical for nutrient supply during plant tissue invasion (Solomon et al. 2003). During conidial germination and the penetration stage, the fungus is nutrient starved in the low-nutrient environment of the plant surface, so metabolism of carbohydrates and lipids in the conidium provide the energy for germination and penetration (Divon and Fluhr 2007; Foster et al. 2016; Voegele et al. 2005). In *Magnaporthe grisea*, the *CPKA/SUM*-encoded PKA holoenzyme controls the mobilization and degradation of stored lipid and glycogen in the penetration structure, the appressorium, which directs the turgor generation, and is required for fungal colonization and pathogenicity (Thines et al. 2000). During spore germination and penetration, fungi mainly decompose the stored lipids through fatty acid metabolism to produce acetyl-coenzyme A (CoA), that is incorporated in the tricarboxylic acid (TCA) cycle by way of the anabolic glyoxylate cycle (Divon and Fluhr 2007).

The mitochondrial α-oxoglutarate dehydrogenase complex (OGDC) consists of three components: oxoglutarate dehydrogenase (OGDH), dihydrolipoyl succinyl transferase (DLST), and dihydrolipoyl dehydrogenase (DLD) (Bunik and Fernie 2009; Gibson et al. 2005; Voet et al. 2016). OGDC, a rate-limiting enzyme system, catalyzes the oxidative decarboxylation of α-oxoglutarate in the TCA cycle, which plays crucial roles in energy production, nitrogen assimilation, and amino acid metabolism (Voet et al. 2016). The TCA cycle fundamentally regulates CO_2 sensing, hyphal growth, and virulence of *Candida albicans* (Tao et al. 2017). Moreover, the side reactions of OGDC also participate in glyoxylate utilization and glutamate signaling (Bunik and Fernie 2009). Isocitrate dehydrogenase, malate dehydrogenase, and pyruvate dehydrogenase are the main enzymes involved in the glyoxylate cycle, which is crucial for NADH metabolism (Voet et al. 2016). Isocitrate lyase and malate synthase are also principal enzymes in the glyoxylate cycle and involved in the virulence of the bacterial pathogen *Mycobacterium tuberculosis* (McKinney et al. 2000), the human pathogenic fungus *C. albicans* (Lorenz and Fink 2001), and the plant pathogenic fungi *M. grisea* (Wang et al. 2003) and *Stagonospora nodorum* (Solomon et al. 2004). *C. albicans* mutants lacking *Isocitrate lyase* (*ICL1*) were markedly less virulent than the wild-type strain in mice (Lorenz and Fink 2001). In *M. grisea*, isocitrate lyase regulates appressorium development and fungal virulence (Wang et al. 2003). Spore germination of *S. nodorum* (Solomon et al. 2004), *Aspergillus nidulans*, and *Neurospora crassa* (Sandeman et al. 1991) is regulated by malate synthase activity. Thus, the TCA cycle not only provides energy, but also regulates biological processes such as hyphal growth and fungal virulence.

The potential roles of α-oxoglutarate dehydrogenase of *V. dahliae*, encoded by *VdOGDH* (VDAG_10018), in energy metabolism, fungal growth, and pathogenicity of *V. dahliae* have not been reported yet. To explore the function of *VdOGDH*, we generated *ΔVdOGDH* gene deletion mutants and corresponding complementary mutants (*ΔVdOGDH-C*) and (1) revealed that *VdOGDH* played a significant role in carbon utilization, conidial and hyphal morphology; (2) confirmed that *VdOGDH* was indispensable in the fungal response against oxidative stress; and (3) showed that *VdOGDH* is involved in the regulation of energy metabolism

and melanin and that (4) virulence of *ΔVdOGDH* strains in cotton was severely reduced.

Materials and methods

Fungal strain and plant material

The wild-type strain (V991) of *V. dahliae* (Vd-wt) was kindly provided by Professor Guiliang Jian from The Institute of Plant Protection, Chinese Academy of Agricultural Sciences (IPP, CAAS) and fungal spores were stored in 25% glycerol at −70 °C. Seeds of Coker 312 cotton were provided by Professor Gaili Jiao from Cotton Research Institute, Shanxi Academy of Agricultural Sciences (Wang et al. 2017).

Constructions of plasmids

Homologous recombination was used to generate *ΔVdOGDH* mutants. The knockout plasmid pGKO-*VdOGDH* was generated as described previously (Qi et al. 2018; Su et al. 2017). Genomic DNA of *V. dahliae* was extracted with the DNAsecure Plant Kit (TIANGEN, Beijing, China) as per the manufacturer's instructions. Flanking fragments, about 1 kb upstream and downstream of the *VdOGDH* gene from the *V. dahliae* genomic DNA, were amplified with primers OGDH-5F/5R and OGDH-3F/3R (Table 1), respectively. The geneticin-resistance cassette (*neo*) was amplified from plasmid pCAM-neo with primers neo-F/neo-R (Table 1). Plasmid pGKO2 (Khang et al. 2005) was digested with HindIII and EcoRI restriction enzymes. Flanking fragments and *neo* were inserted into linearized vector pGKO2 (Fig. S1) using the In-Fusion enzyme (Clontech, Mountain View, CA, USA).

For constructing the complementary plasmid pCM-Hyg-*VdOGDH*, TrpC promoter (amplified with primers TrpC-F/TrpC-R, Table 1), complementary DNA (cDNA) of *VdOGDH*, and Nos terminator (amplified with primers Nos-F/Nos-R, Table 1) were inserted into linearized vector pCM-Hyg, which carried the hygromycin B resistance cassette (*hph*) and was double digested with HindIII and XbaI enzymes. The TrpC promoter and Nos terminator were amplified from plasmid pCH-GFP (Xu et al. 2013).

Fungal transformation and mutant confirmation

The *VdOGDH* knockout mutants were generated by transferring the knockout plasmid pGKO-*VdOGDH* into protoplasts isolated from Vd-wt using PEG-mediated transformation as described previously (Rehman et al. 2016). Protoplasts of *ΔVdOGDH* mutants were similarly transformed with the complementary plasmid pCM-Hyg-*VdOGDH* to obtain the complementary mutants (*ΔVdOGDH-C*).

Mutants were preliminarily selected using antibiotic stress and single-spore isolation, then confirmed by genomic PCR using specific primers. *ΔVdOGDH* mutants were selected on potato dextrose agar (PDA) in the presence of geneticin (G418, 50 μg/mL) and confirmed by PCR with primers neo-F/neo-R and OGDH-F/OGDH-R (Table 1). *ΔVdOGDH-C* mutants were cultured and selected on PDA plates containing hygromycin B (50 μg/mL). Primers Hyg-F/Hyg-R (Table 1) and OGDH-F/OGDH-R were used for genomic PCR to check whether the complementation was successful.

Table 1 Primers used for mutant construction and confirmation

Primer	Primer sequence
neo-F	GTTTGCGGGCTGTCTTGACG
neo-R	TACCTGTGCATTCTGGGTAA
OGDH-5F	GTACCCAATTC***GAATTC***GAGAAGAACTCGCAACGAC
OGDH-5R	CAAGACAGCCCGCAAACGGGTTTGTCTAAAGGAGGGA
OGDH-3F	CCCAGAATGCACAGGTAAAGTGGTTTGGACCTGGC
OGDH-3R	GACGGTATCGAT***AAGCTT***ATGCGAACGGGCTTGATG
OGDH-C-F	ATGCTGCGCAGCTCGCTGAGCAAAG
OGDH-C-R	TCAGCACAAGCAAGATATTGAGGGG
TrpC-F	GTAATCCTTCTT***TCTAGA***TTGAAGGAGCATTTTTGGGC
TrpC-R	CAGCGAGCTGCGCAGCATATCGATGCTTGGGTAGAATAGG
Nos-F	ATATCTTGCTTGTGCTGAATCCACTTAACGTTACTGAAATC
Nos-R	ACGGCCAGTGCC***AAGCTT***AACATGCAATTATCTTTGCG
OGDH-F	ACGAGCAGAAGGGCTTTGGTA
OGDH-R	TGGCAGACGAAGTTGACGG
Hyg-F	TTGAAGGAGCATTTTTGGGC
Hyg-R	TTATCTTTGCGAACCCAGGG

Bold and italicized sequences are restriction enzyme cleavage sites

Growth of mutants on different carbon sources

Vegetative growth of the Vd-wt, *ΔVdOGDH*, and *ΔVdOGDH-C* strains on different media was then compared. Each strain was first cultured in complete medium (CM) (Qi et al. 2018), and was then filtered through a sterile 40 µm Falcon Cell Strainer (New York, NY, USA) to collect conidia. A drop of a conidial suspension (10 µL, 2×10^6 spores/mL) of the respective strains was placed in the center of a plate of Czapek Dox agar with sucrose (30 g/L) and without sucrose, pectin (10 g/L), xylose (10 g/L), starch (17 g/L) or galactose (10 g/L) (Qi et al. 2016). A 10 µL drop of a conidial suspension (2×10^6 spores/mL) was also placed in the center of PDA plates. The plates were incubated at 25 °C in the dark. Each strain was tested on five plates of each source. Colony morphology was photographed and diameters were measured after 14 days. The mean colony diameter of Vd-wt was compared with that of the *ΔVdOGDH* and *ΔVdOGDH-C* strains for each of the carbon sources tested. The experiment was repeated two times.

A 100 µL drop of conidial suspension (5×10^6 spores/mL) of the respective strains was evenly spread on a plate of basal modified medium (BMM, 0.2 g/L $NaNO_3$, 0.52 g/L KCl, 0.52 g/L $MgSO_4{\cdot}7H_2O$, 1.52 g/L KH_2PO_4, 3 µmol/L thiamine, 0.1 µmol/L biotin, 5 g/L glucose, 15 g/L agar) (Bai et al. 2011). The plates were incubated at 25 °C in the dark for 30 days, then colony morphology and microsclerotial production were examined.

Conidial production and microscopic observation of conidia and hyphae

A conidial suspension (1 mL, 5×10^6 spores/mL) of Vd-wt, *ΔVdOGDH* or *ΔVdOGDH-C* strains was added to 200 mL Czapek Dox broth in sterile conical flasks. After 6 days on a shaker at 180 rpm and 25 °C, the suspension was filtered through a cell strainer, and then the conidia were counted using a hemacytometer and light microscope. Conidia production was then calculated as previously described (Qi et al. 2018).

A drop of the conidial suspension of Vd-wt and *ΔVdOGDH* strains (*ΔVdOGDH-1* and *ΔVdOGDH-2*) from the previous step was also spread evenly on PDA plates and incubated as described. After 5 days, 5 mL sterile water was added to the plates, then the agar was gently scraped with a sterile spreader to collect the conidia as described. Conidia were then observed with an Axio Imager M2 microscope (Zeiss, Jena, Germany).

For examining hyphal characteristics of Vd-wt and *ΔVdOGDH* strains, the method (Yang et al. 2009) was used with a slight modification. Conidia (2 µL, 10^5 spores/mL) were placed in 20 µL liquid CM on a clean microscope slide, which was then incubated on filter paper moistened with sterile water in a Petri dish. After 48 h at 25 °C in the dark, any hyphae were then observed with the light microscope.

For high-quality imaging of conidial and hyphal morphology, conidia and hypha were washed with PBS buffer (pH 7), then stained with 5 µg/mL Calcofluor white (CFW). After 10 min, the stain was washed away with PBS buffer. Fluorescence was observed with a confocal laser scanning microscope (CLSM) LSM 700 (Zeiss, Jena, Germany) using 345 nm excitation wavelength and band-pass 420–470 nm emission filters.

Oxidative stress assay and intracellular ROS levels detection

Oxidative stress was assayed using the method of previous research (Rehman et al. 2017). A conidial suspension (500 µL, 5×10^6 spores/mL) of each strain was spread evenly on Czapek Dox plates. Then 100 µL H_2O_2 (100 mM) was poured into a hole punched by a sterile cork borer (∅ = 5 mm) in the center of the plate. Plates were incubated at 25 °C, and the diameter of the inhibition zone was measured after 7 days. Each strain was tested on five plates, and the assay was done three times.

For intracellular ROS detection, conidia (2 µL, 10^4 spores/mL) of the respective strains were added to 20 µL CM broth at 25 °C for 3 days, then ROS levels generated by each strain were qualitatively tested using a Reactive Oxygen Species Testing Kit (GENMED Scientific Inc., Shanghai, China) and the lit protocol. Green fluorescence of hyphae of strains Vd-wt and *ΔVdOGDH* was observed with the LSM 700 using 488 nm excitation wavelength and band-pass 500–550 nm emission filters.

Expression analysis of related genes

To further investigate whether disruption of *VdOGDH* triggers sensitivity to oxidative stress, the relative expression levels of the glutathione reductase (VDAG_07524.1), gamma-glutamylcysteine *synthetase* (VDAG_00135.1), and thioredoxin (VDAG_03464.1) genes, involved in the oxidative response, were quantified (Han et al. 2015).

To study the impact of *VdOGDH* disruption on the regulation of other genes related to energy metabolism, we analyzed the transcript levels for genes encoding the main enzymes involved in the glyoxylate cycle: isocitrate lyase (VDAG_08615, *VdICL*), isocitrate dehydrogenase (VDAG_00099, *VdICDH*), malate dehydrogenase (VDAG_06317, *VdMDH*), pyruvate dehydrogenase (VDAG_06356, *VdPDH*). We similarly analyzed genes related to melanin and microsclerotia formation (Hu et al. 2014): class II hydrophobin gene (VDAG_02273, *VDH1*), pigment biosynthesis protein

Ayg1 (VDAG_04954, *Vayg1*) (Fan et al. 2017), scytalone dehydratase (VDAG_03393, *VdSCD*) (Luo et al. 2016), laccase (VDAG_00189, *VdLAC*), tetrahydroxynaphthalene reductase (VDAG_03665, *VT4HR*), and versicolorin reductase (VDAG_00183, *VaflM*) (Duressa et al. 2013).

Conidia were harvested from a 6-day-old culture of Vd-wt, *ΔVdOGDH*, and *ΔVdOGDH-C* strains and the concentration was adjusted to 10^6 spores/mL. One microliter of the respective suspensions was inoculated in 200 mL of CM and incubated on the shaker (180 rpm) at 25 °C. After 5 days, the culture was filtered through four layers of clean gauze to collect hyphae. Total RNA was extracted from the respective hyphae using the RNA Extraction Kit (YPHBio, Tianjin, China). First strand cDNA was synthesized with TransScript One Step gDNA Removal and cDNA Synthesis Kit (TransGen Biotech, Beijing, China) according to the instructions. qRT-PCR was performed using TransStart Tip Green qPCR SuperMix (TransGen Biotech, Beijing, China).

The respective primer sequences used for amplification are listed in Table 2. The housekeeping gene actin (VDAG_00941) was used for normalization and amplified with primers Vd-A-F/Vd-A-R (Table 2). Expression of the respective genes was analyzed by qRT-PCR using an ABI7500 Fast Real-Time PCR System (Applied Biosystems, USA) with the following process: holding stage, 94 °C for 30 s; cycling stage, 94 °C for 5 s, 60 °C for 34 s, 72 °C for 10 s, 40 cycles; and melt curve stage, 95 °C for 15 s, 60 °C for 1 min, 95 °C for 30 s, 60 °C for 15 s. The experiment was independently repeated two times, and relative expression ratio was calculated by the $2^{-\Delta\Delta Ct}$ method (Livak and Schmittgen 2001).

Pathogenicity assay of *VdOGDH* deletion mutants

Coker 312 seeds were sown in bottomless paper cups (Zhu et al. 2013) filled with autoclaved soil mix (1:1, vermiculite:humus). The cups were placed on plastic trays

Table 2 Primers used for relative gene expression and fungal biomass assays

Primer	Primer sequence	Target gene
Vd-A-F	GTCCATCTTGCCCTCTTTCCA	Actin
Vd-A-R	TCCCTCACCTTCCTTCGGAT	
ICDH-F	TTGCTCTCCCGCATCTGGC	*ICDH*
ICDH-R	CACTTGACGCCGACGCTGT	
PDH-F	AACTTCTACGGCGGCAAC	*PDH*
PDH-R	CCTCAAAGACCTGACCCTG	
MDH-F	CGCTGCCGAGGTTCTCAA	*MDH*
MDH-R	GCCAGAGTGACCACCGAT	
ICL-F	CATCAGCGACAAGTTTGCCC	*ICL*
ICL-R	GCTACATCATACCACTCTACTGCT	
VaflM-F	GACTGTCAATGCCATCGCC	*VaflM*
VaflM-R	CGGTGACCTTGATAACTT	
VdSCD-F	ATGCCCGCTTCCGAGTTC	*VdSCD*
VdSCD-R	TTCCACACGCCGTCAATCTT	
VdLAC-F	CGTTTCCTCACTTTAGCCACAGC	*VdLAC*
VdLAC-R	CACCCAGTCCACCGTCCATTTGT	
VT4HR-F	TGGTGGCATCAAGACAGACA	*VT4HR*
VT4HR-R	CGAAGCGAGGAAGCAAACAA	
Vayg1-F	GTTGCGACGAGTTCTTGT	*Vayg1*
Vayg1-R	ACCATCACCTTGCCCATA	
VDH1-F	GTCTATTCATCTGGTTCCTCCCTA	*VDH1*
VDH1-R	CAAACCTCTTACAATGTTGACGC	
VD_07524.1-F	AACATTCCCTCGGTCGTCTT	Glutathione reductase
VD_07524.1-R	TGGCGGTGAACTTGGTCTT	
VD_00135.1-F	AATCCACGAATTGGCAGCACA	Gamma-glutamyl-cysteine synthetase
VD_00135.1-R	CGGGTTACCAGCACCATGAAGA	
VD_03464.1-F	CGCCATGCCGACCTTTGT	Thioredoxin
VD_03464.1-R	CGACGAGCCCATCACCAGA	
SSU-F	AACTTAAAGGAATTGACGGAAG	*SSU*
SSU-R	GCATCACAGACCTGTTATTGCC	

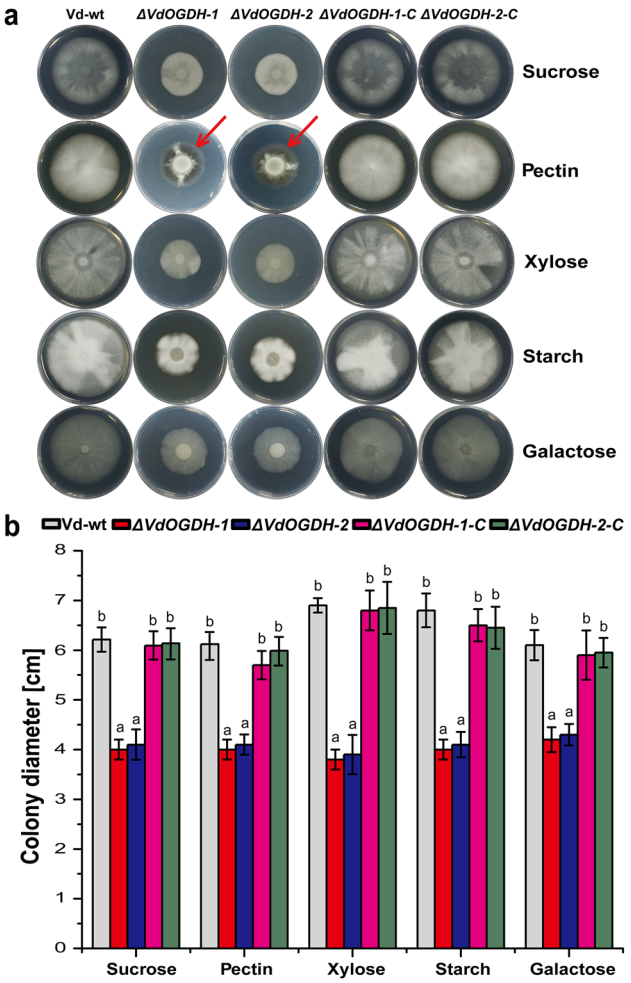

Fig. 1 Vegetative growth assay. Colonies and diameter of Vd-wt, *ΔVdOGDH* strains, and *ΔVdOGDH-C* strains of *V. dahliae* grown on Czapek Dox agar amended with different carbon sources. **a** Phenotypes and **b** mean (±SD) colony diameters of each strain after 14 days. The experiment was done three times for each carbon source. Different letters above bars for a carbon source indicate a significant difference among strains ($P < 0.05$)

and then kept in a growth chamber at 25–28 °C, with 16 h photoperiod and 50–60% relative humidity. Each fungal strain was cultured in CM for 7 days, and respective conidia were collected by centrifugation for 10 min at 6000 rpm, and the concentration was adjusted to approximately 5×10^7 spores/mL. Seedlings with 4–5 leaves were inoculated with a conidial suspension by placing the paper cups onto a Petri dish (∅ = 90 mm) containing 10 mL of a conidial suspension for 10 min. The control group was treated with sterile water. The plants were then returned to the chamber, and the disease severity was assessed at 30 days after inoculation (dpi), and then disease index was evaluated as described previously (Rehman et al. 2017). Each fungal strain was tested on five cups of plants (15–20 plants total for each strain). The experiment was done three times.

Fungal biomass assay

To qualitatively evaluate any difference in virulence among the Vd-wt and mutant strains, we cut off the stems of the cotton seedlings used in the pathogenicity assay to check for vascular discoloration (Xiong et al. 2015) at 30 dpi and placed a stem piece onto PDA plates to isolate any hyphae from vascular bundles (Qi et al. 2016; Zhao et al. 2017).

We also used qRT-PCR to quantify fungal biomass in the cotton seedlings. At 21 dpi, total genomic DNA was extracted from roots and leaves of test plants using the DNAsecure Plant Kit (TIANGEN, Beijing, China). The qRT-PCR reactions were carried out using TransStart Top Green qPCR Supermix (TransGen Biotech). Cotton small subunit ribosomal RNA gene (*SSU*) was selected as a standard control (Hao et al. 2018) and amplified with primers SSU-F/SSU-R (Table 2). *V. dahliae actin* gene (VDAG_00941) was amplified with primers Vd-A-F/Vd-A-R (Table 2) to quantify fungal DNA in the mixed DNA samples.

Statistical analysis

Data are presented as mean ± standard deviation (SD), and means were statistically compared among treatments or strains using Duncan's multiple range tests in SPSS statistics 17.0 software (SPSS, Chicago, USA). Differences were considered statistically significant at $P < 0.05$.

Results

Deletion and complementation of *VdOGDH* in *V. dahliae*

In *VdOGDH* gene deletion mutants, *VdOGDH* gene was replaced using the neomycin resistance cassette in the gene construct (Fig. S1). With gene replacement or T-DNA random insertion in V991, geneticin resistance should be introduced into the transformants. Gene deletion mutants were preliminarily selected and confirmed in the presence of geneticin. Ectopic transformants were excluded, and deletion mutants were confirmed by genomic PCR with primers OGDH-F/OGDH-R for 4 of 24 transformants analyzed by PCR (Fig. S2a, b). *ΔVdOGDH-1* and *ΔVdOGDH-2* were randomly selected for further analysis.

With transformations using the complementary plasmid pCM-Hyg-*VdOGDH*, a functional copy of *VdOGDH* was inserted into *ΔVdOGDH* mutants and complementary strains were (*ΔVdOGDH-C*) generated. Successful transformation was confirmed by genomic PCR with primers Hyg-F/Hyg-R and OGDH-F/OGDH-R (Fig. S2c, d). *ΔVdOGDH-1-C* and *ΔVdOGDH-2-C* were selected for further phenotypic observations.

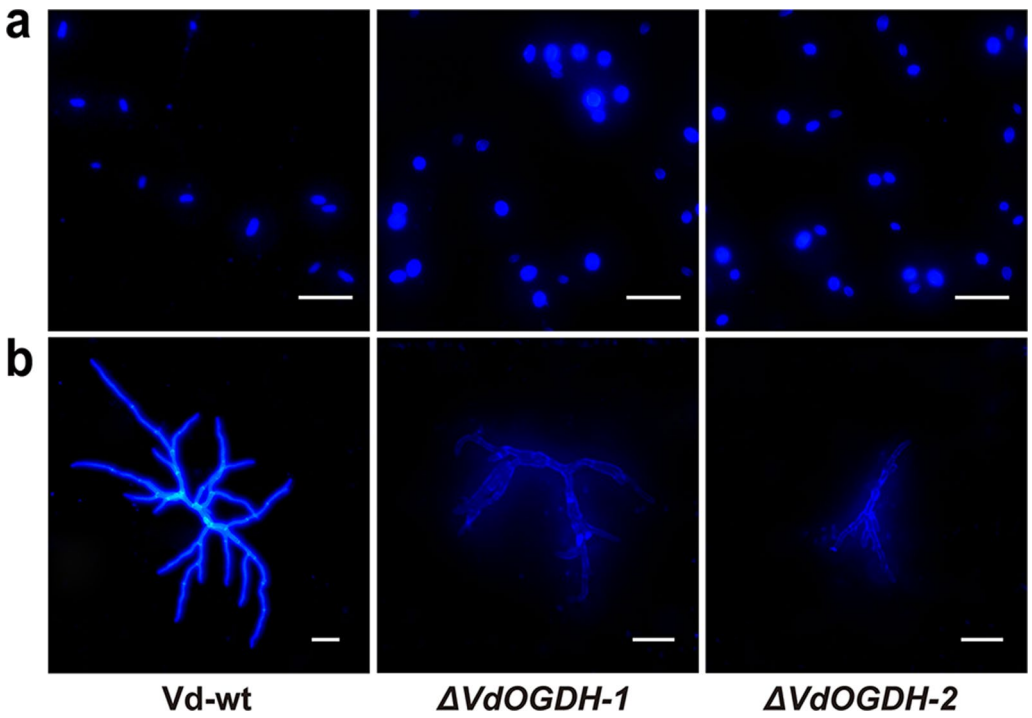

Fig. 2 Morphology of conidia and hyphae of Vd-wt and *ΔVdOGDH* strains stained with Calcofluor white (CFW) and viewed with a confocal laser scanning microscope. **a** Conidia after 5 days on PDA plates. Conidia of *ΔVdOGDH-1* and *ΔVdOGDH-2* were round or spherical, rather than the typical oblong or elliptic shape **b** Hyphae of each strain after 24 h. *ΔVdOGDH* strains branched irregularly and did not form whorled branches. The hyphae of *ΔVdOGDH* strains were also more swollen than those of Vd-wt. Bars: 20 µm

Vegetative growth of *ΔVdOGDH* mutants was significantly impaired

To analyze the function of *VdOGDH* on mycelial growth and carbon utilization, we compared radial growth rates of the Vd-wt and mutants on PDA plates and Czapek Dox agar amended with different carbon sources (sucrose, pectin, xylose, starch, and galactose). There was no significant difference in the growth rate of the strains on PDA, but the aerial hyphae of *ΔVdOGDH* strains was underdeveloped compared with those of Vd-wt and *ΔVdOGDH-C* strains (Fig. S3a, b). Vd-wt and complementary strains (*ΔVdOGDH-1-C* and *ΔVdOGDH-2-C*) cultured on pectin and starch had more extensive aerial hyphae (Fig. 1a). In contrast, strains *ΔVdOGDH-1* and *ΔVdOGDH-2* produced melanin on pectin-containing plates, as indicated by the arrows (Fig. 1a). In addition, the corresponding mean colony diameters of *ΔVdOGDH-1* (4.0 cm, 4.0 cm, 3.8 cm, 3.9 cm, 4.2 cm) and *ΔVdOGDH-2* (4.1 cm, 4.1 cm, 3.9 cm, 4.1 cm, 4.3 cm) on Czapek Dox agar plates supplied with different carbon sources (sucrose, pectin, xylose, starch, and galactose) were significantly smaller than those of Vd-wt (6.2 cm, 6.1 cm, 6.9 cm, 6.8 cm, 6.1 cm), *ΔVdOGDH-1-C* (6.1 cm, 5.7 cm, 6.8 cm, 6.5 cm, 5.9 cm), and *ΔVdOGDH-2-C* (6.2 cm, 6.1 cm, 6.8 cm, 6.5 cm, 5.9 cm) (Fig. 1b). These phenomena indicate that *VdOGDH* is important for vegetative growth and carbon utilization of *V. dahliae*.

Knockout of *VdOGDH* reduced conidial production and caused abnormal morphology of conidia and hyphae

To confirm the effect of *VdOGDH* knockout on conidial production, we evaluated conidiophores production of each strain further. After 6 days in Czapek Dox broth, the *ΔVdOGDH* strains produced significantly fewer conidia than the Vd-wt and *ΔVdOGDH-C* strains did (Fig. S3c). Thus, *VdOGDH* contributes to conidiation.

When conidia and hyphae were observed with the optical microscope after CFW staining, conidia of *ΔVdOGDH-1* and *ΔVdOGDH-2* from 5-day-old cultures were round or spherical, rather than the typical oblong or elliptical shape of the Vd-wt (Fig. 2a, S4a). After 24 h of culturing, Vd-wt hyphae displayed radical and fast growth; however, *ΔVdOGDH* strains hyphae grew slowly and generated swollen and atypical branches (Fig. 2b). After culturing for 48 h on slides, the hyaline hyphae of Vd-wt had developed typical whorled branches, and conidia had formed at the tip of the hyphae (Fig. S4b), whereas hyphae of strains *ΔVdOGDH-1* and *ΔVdOGDH-2* branched irregularly and did not form whorled branches. Hyphae of the *ΔVdOGDH* strains were

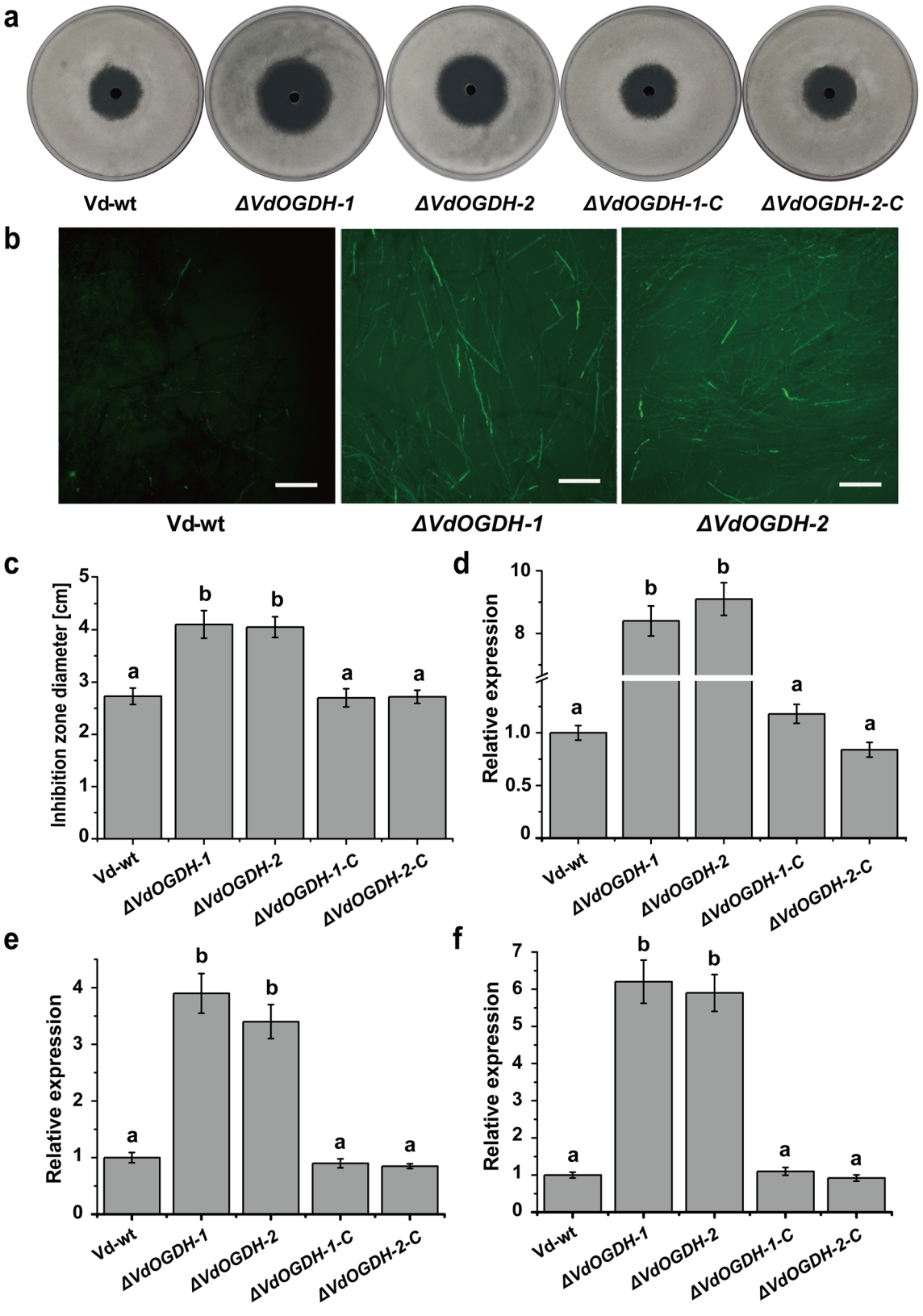
a
Vd-wt
ΔVdOGDH-1
ΔVdOGDH-2
ΔVdOGDH-1-C
ΔVdOGDH-2-C
b
Vd-wt
ΔVdOGDH-1
ΔVdOGDH-2
c
Inhibition zone diameter [cm]
d
Relative expression
e
Relative expression
f
Relative expression

◂**Fig. 3** Oxidative stress assay, intracellular ROS level detections, and expression levels of oxidative stress response genes in Vd-wt, *ΔVdOGDH*, and *ΔVdOGDH-C* strains. **a** Inhibition zones after 1 week in oxidative stress assay. For each strain, 500 conidia in suspension (5×10^6 spores/mL) were spread evenly on the Czapek Dox plates. 100 µL H_2O_2 (100 mM) was poured into a hole in the center of the plate. **b** ROS levels in hyphae from 3-day-old CM culture. Hyphae were stained with the Reactive Oxygen Species Testing Kit, and viewed with confocal microscopy. Bars: 50 µm. **c** Mean (±SD) diameter of H_2O_2 inhibition zone diameter. Three independent replicates were done. Different letters above the bars indicate a significant difference among treatment groups ($P<0.05$). **d**–**f** Mean (±SD) gene expression analysis. Conidia harvested from the plates were cultured in CM for RNA extraction. qRT-PCR reactions were perform using specific primers. The experiment was done three times. Different letters above bars indicate a significant difference among strains ($P<0.05$). The expression levels of **d** glutathione reductase (VDAG_07524.1), **e** gamma-glutamylcysteine synthetase (VDAG_00135.1) and **f** thioredoxin (VDAG_03464.1) were detected

also more swollen than those of Vd-wt, and no spores were formed from the tip of branches (Fig. S4b). These results show that knockout of *VdOGDH* inhibits the spore morphology and mycelial development.

Deletion of *VdOGDH* resulted in increased susceptibility to oxidative stress

The sensitivity of each strain to exposure to H_2O_2 was checked by measuring the diameter of any inhibition zone. The zone of inhibition for *ΔVdOGDH-1* and *ΔVdOGDH-2* strains was larger than for the wild type and complementary strains (Fig. 3a, S4b). We further measured intracellular ROS levels of each strain. As expected, *ΔVdOGDH* mutants showed brighter green fluorescence (Fig. 3b), which meant the intracellular ROS levels were higher in *ΔVdOGDH* mutants than in Vd-wt. The deletion of *VdOGDH* resulted in increased expression of the genes related to the oxidative response. Genes for glutathione reductase, gamma-glutamylcysteine synthetase, and thioredoxin increased by approximately ninefold, fourfold, sixfold, respectively, in *ΔVdOGDH* mutants than in Vd-wt and *ΔVdOGDH-C* strains (Fig. 3c–e). The increased expression of these genes may be indicative of the higher level of ROS in *ΔVdOGDH* mutants.

VdOGDH related to energy metabolism

In the qRT-PCR of metabolic genes, the transcript level of *VdICL* increased about 11-fold in *ΔVdOGDH* mutants compared with the Vd-wt and *ΔVdOGDH-C* strains (Fig. 4a). Deletion of *VdOGDH* also resulted in significantly increased expression of *VdICDH*, *VdMDH*, and *VdPDH* compared with levels in the Vd-wt and complementary strains (Fig. 4b–d). This increased expression suggests that *VdOGDH* is critical for energy metabolism in *V. dahliae*.

Deletion of *VdOGDH* resulted in increased microsclerotia production and expression of genes related to melanin and microsclerotia production

Due to different melanin production of *ΔVdOGDH-1* and *ΔVdOGDH-2* strains (indicated by arrows) on pectin-containing Czapek Dox agar (Fig. 1a), we, therefore, checked for microsclerotia production and the expression level of microsclerotia formation-related genes. After growth on BMM, *ΔVdOGDH* strains produced many more microsclerotia than did Vd-wt and *ΔVdOGDH-C* strains (Fig. 5a). As expected, expression of *VaflM*, *Vayg1*, *VT4HR*, *VdLAC*, and *VdSCD* increased in the melanin-producing *ΔVdOGDH* mutants, about 2.0-, 2.0-, 3.2-, 3.2- and 3.7-fold more, respectively, than in the Vd-wt and *ΔVdOGDH-C* strains (Fig. 5b, c, e–g). The expression level of genes related to melanin formation in *ΔVdOGDH* strains was significantly higher than that of Vd-wt and *ΔVdOGDH-C* strains. In contrast, the expression of *VDH1*, which is involved in the development of microsclerotia (Klimes and Dobinson 2006), however, did not obviously differ among Vd-wt, *ΔVdOGDH*, and *ΔVdOGDH-C* mutants (Fig. 5d). Thus, *VdOGDH* gene is apparently involved in the production of melanin and microsclerotia in *V. dahliae*.

VdOGDH is essential for full virulence in *V. dahliae*

In the virulence test on cotton seedlings, at 30 dpi, cotton plants irrigated with water were growing well without any wilting, but the seedlings inoculated with *V. dahliae* strains all had different degrees of characteristic disease symptoms (Fig. 6a, b). Severe leaf chlorosis and necrosis, stunting, and even death were apparent on cotton plants inoculated with Vd-wt and *ΔVdOGDH-C* strains. In spite of the wilt symptoms on plants inoculated with *ΔVdOGDH* strains, plants developed only mild leaf chlorosis; no plants became necrotic (Fig. 6a). As expected, cotton plants inoculated with Vd-wt and *ΔVdOGDH-C* strains had browned stems, whereas only a few vascular bundles had browned slightly in plants infected with *ΔVdOGDH* strains (Fig. 6b). Furthermore, fewer fungal colonies grew from excised stem sections of seedlings inoculated with the *ΔVdOGDH* strains than with Vd-wt or *ΔVdOGDH-C* strains (Fig. 6c).

The disease index for plants infected by Vd-wt and *ΔVdOGDH-C* strains was significantly higher than for those inoculated with *ΔVdOGDH* strains (Fig. 6d). When the fungal biomass in roots and leaves was evaluated by qRT-PCR to assess the role of *VdOGDH* in systemic infection, the biomass of the *ΔVdOGDH* strains was always significantly lower than that of Vd-wt and *ΔVdOGDH-C* strains, whereas the biomass of Vd-wt and *ΔVdOGDH-C* strains did not differ significantly (Fig. 6e, f). Thus, the *VdOGDH* deletion attenuated fungal virulence in cotton plants.

Discussion

Carbon catabolism provides energy for fungi during plant infection (Solomon et al. 2003) and is required for fungal development and closely related to pathogenicity. The F-box protein Frp1 is essential for sexual reproduction and carbon source utilization in *Fusarium graminearum* and *Botrytis cinerea*, and FgFRP1 regulates the infection of barley roots by *F. graminearum*, but not infection of aerial plant parts (Jonkers et al. 2011). *Aspergillus* fungi can convert and utilize different sugar monomers in the plant as carbon sources for a variety of catabolic pathways that all are connected to glycolysis (Khosravi et al. 2015). In *Pyricularia oryzae*, glycerol-3-phosphate dehydrogenases, PoGpd1 and PoGpd2, important cellular redox enzymes, played essential physiological roles in hyphal differentiation, utilization of carbon sources, and virulence (Shi et al. 2018). OGDC is located in the mitochondrial matrix and catalyzes the decarboxylation of α-ketoglutarate to produce succinyl CoA with the reduction of NAD^+ to generate NADH, which is critical for energy metabolism (Bunik and Fernie 2009). In *Saccharomyces cerevisiae*, *KGD1* and *KGD2* encode the OGDH and DLST components, independently, of the OGDH. Mutants with a *KGD1* or *KGD2* gene deletion can grow on minimal medium containing glucose, but not grow on a medium with glycerin as the sole carbon (Repetto and Tzagoloff 1989; Repetto and Tzagoloff 1990). In our study, due to a deletion in *VdOGDH*, vegetative growth and conidial production were significantly impaired in *ΔVdOGDH* mutants compared with Vd-wt and complementary strains. When all strains were cultured on PDA plates, there was no obvious difference of growth rates among the strains. However, when all strains were cultured on Czapek Dox agar containing different carbon sources, colony diameters of *ΔVdOGDH* mutants were obviously smaller, and conidia and hyphae were abnormal, with rounded or spherical shape spores and irregularly branched mycelia. The phenotypic characteristics, thus, suggest that *VdOGDH* is involved in carbon utilization and vegetative growth of *V. dahliae*.

The two-carbon compounds, acetic acid and ethanol, can be utilized as the main carbon sources and assimilated into the TCA cycle through the glyoxylate bypass (Voet et al. 2016). Generally, induction of the glyoxylate cycle indicates that lipid metabolism, including β-oxidation and acetyl CoA production is the major process for energy production in the fungal cell (Wang et al. 2003) and early stage of conidial germination and infection by plant pathogenic fungi (Divon and Fluhr 2007). Two L-lactate dehydrogenase in *Fusarium graminearum* (*FgLDHL1* and *FgLDHL2*) are involved in the utilization of carbon sources and energy production during spore germination (Chen et al. 2018b). Lipid stores are mobilized through lipolysis and β-oxidation to form acetyl-CoA, which is further assimilated into the TCA cycle via the glyoxylate cycle in the plant pathogen *Tapesia yallundae* during infection (Bowyer et al. 2000). During appressorium and invasive hyphae formation in the rice blast fungus *M. grisea*, expression of the isocitrate lyase gene *ICL1* is high (Wang et al. 2003). In our research, decarboxylation of α-ketoglutarate in the TCA cycle may be disturbed because of the deletion of *VdOGDH*. Considering the significant role of isocitrate lyase in the glyoxylate cycle, the upregulated transcript level of *VdICL* in the deletion mutants indicates that the glyoxylate cycle may be more active in *ΔVdOGDH* mutants. In addition, other enzyme-encoding genes involved in the glyoxylate cycle (*VdICDH* and *VdMDH*) and in the TCA cycle (*VdPDH*) were unregulated in *ΔVdOGDH* strains, indicating that the glyoxylate cycle may partially complement the disruption of the TCA cycle in *ΔVdOGDH* mutants.

Lipid droplets are transferred from the conidium to the incipient appressorium, where triacylglycerol lipase is present and critical for appressorium maturation in *M. grisea* (Thines et al. 2000). In addition to providing energy for spore germination and infection structure formation (Wang et al. 2003), lipid metabolism can also provide energy for secondary metabolic processes, such as melanin production (Solomon et al. 2004; Wang et al. 2003). In *V. dahliae*, the presence of dense black melanin deposits was regarded as one main characteristics of microsclerotia formation (Butler and Day 1998). Melanized microsclerotia, which can survive in the soil for more than 10 years without a host, serve as survival structures for *V. dahliae* (Klosterman et al. 2009). The molecular mechanism of melanin biogenesis and structural formation of microsclerotia, however, are still unclear (Duressa et al. 2013; Hawke and Lazarovits 1994; Hu et al. 2014). When cultured on BMM plates, *ΔVdOGDH* strains generated many more microsclerotia than that of Vd-wt and *ΔVdOGDH-C* strains. Melanin was produced by *ΔVdOGDH* strains cultured on the medium containing pectin but not by Vd-wt and complementary strains, and expression levels of genes related to melanin production (*Vayg1*, *VdSCD*, *VdLAC*, *VT4HR*, and *VaflM*) corresponded to the differences in melanin in the strains. We speculate that the increased expression of *VdICL* may cause the enhancement of isocitrate lyase. Metabolic activity in branches of the glyoxylate cycle may also be increased, so that secondary metabolic processes, including melanin synthesis, also increase. But this possibility and the mechanism underlying the increased production of melanin in *ΔVdOGDH* mutants need further research.

Reactive oxygen species are ubiquitous molecules of redox pathways that play an essential role in plant defense mechanism (Kotchoni and Gachomo 2006). Host invasion by pathogens will cause excessive ROS accumulation. This oxidative burst will occur at the invasion sites, causing local cell death

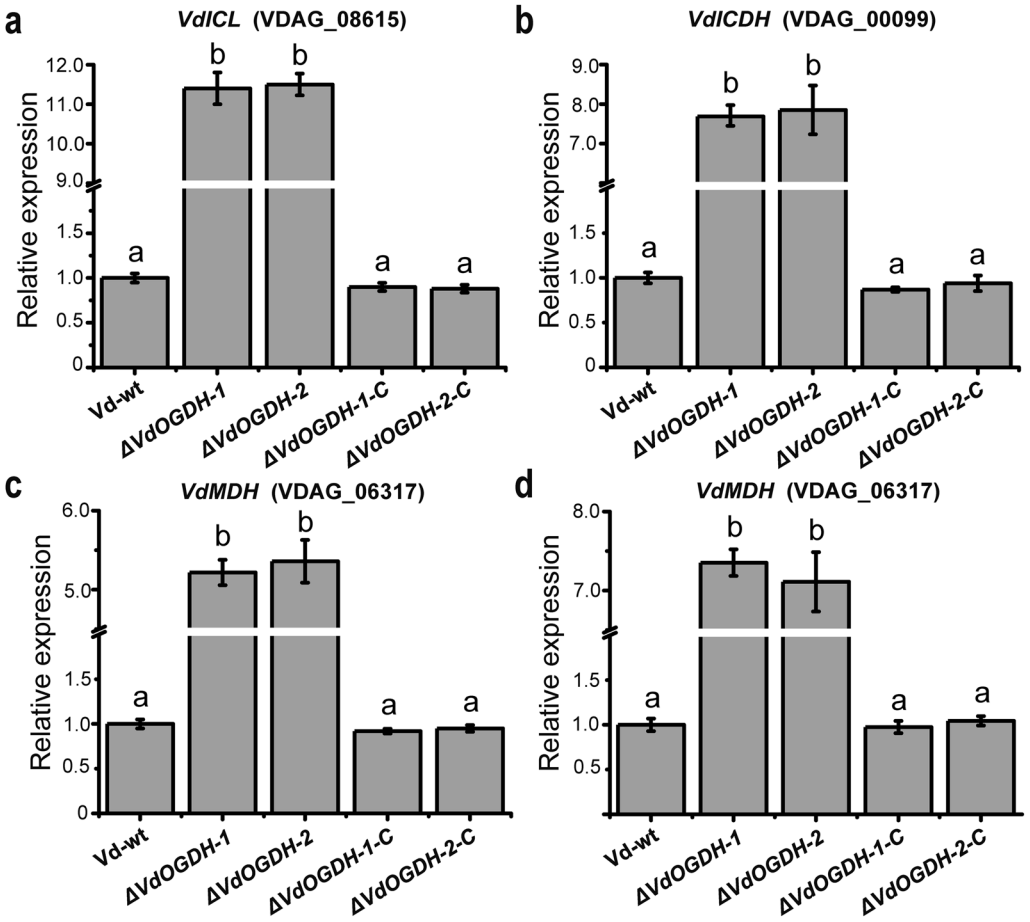

Fig. 4 Mean (±SD) relative expression of genes related to energy metabolism in Vd-wt, *ΔVdOGDH*, and *ΔVdOGDH-C* strains from 5-day-old cultures in CM broth. The expression levels were detected by qRT-PCR with specific primers, respectively. **a** *VdICL* (VDAG_06356), **b** *VdICDH* (VDAG_06356), **c** *VdMDH* (VDAG_06356), and **d** *VdPDH* (VDAG_06356). The experiment was done three times. Different letters above the bars indicate a significant difference among strains ($P < 0.05$)

to limit pathogen invasion (Yun et al. 2011). The adaptability of plant pathogenic fungi to ROS is, thus, a determinant for normal growth and pathogenicity (Klosterman et al. 2011). In *Phytophthora sojae*, the importin α subunit gene *PsIMPA1* mediates the oxidative stress response, and deletion of *PsIMPA1* causes a decrease in fungal adaptability to ROS and ROS detoxification, and subsequently decreased virulence (Yang et al. 2015). During infection, cotton plants also generate a high level of ROS when resisting infection by *V. dahliae* (Luo et al. 2014; Xie et al. 2013; Zhang et al. 2012). In the present oxidative stress assay, the zone of H_2O_2 inhibition for the *ΔVdOGDH-1* and *ΔVdOGDH-2* strains was larger than for the Vd-wt and complementary strains, indicating that deletion of *VdOGDH* caused the increased sensitivity to the oxidative stress. ROS act as an important intracellular messenger for many bioreactions, but high concentration is likely to stress cells (Cadenas and Davies 2000). The deletion of *VdOGDH* led to the increased expression of genes involved in the oxidative response and higher intracellular oxidative stress in *ΔVdOGDH* strains. High sensitivity to ROS would, thus, be a limiting factor for *ΔVdOGDH* strains, which caused milder symptoms and led to a lower disease index than the Vd-wt and *ΔVdOGDH-C* strains did. The lower biomass of the mutant strains in cotton plants also suggests that they may be impaired in their ability to infect and colonize plants. The reduced biomass and virulence of the *ΔVdOGDH* mutants, thus, demonstrate that *VdOGDH* is required for virulence of *V. dahliae*.

To date, some of the vegetative growth and/or pathogenicity-related genes of *V. dahliae* have been identified. Vegetative growth-related genes of *V. dahliae* mainly regulate sporulation, microsclerotial formation, and hyphal growth (Luo et al. 2014), and include a class II hydrophobin gene (*VDH1*) (Klimes et al. 2008; Klimes and Dobinson 2006), glutamic acid-rich protein 1 gene (*Vdgrp1*) (Gao et al. 2010), NPP1 domain-containing protein (*VdNLP*) (Santhanam et al. 2013; Zhou et al. 2012), small GTPase gene *VdRac1* and its interaction partner (*VdCal4*) (Tian et al. 2015), transcription factor (*Vdpf*) (Luo et al. 2016). Genes directly or indirectly related to pathogenicity are linked with

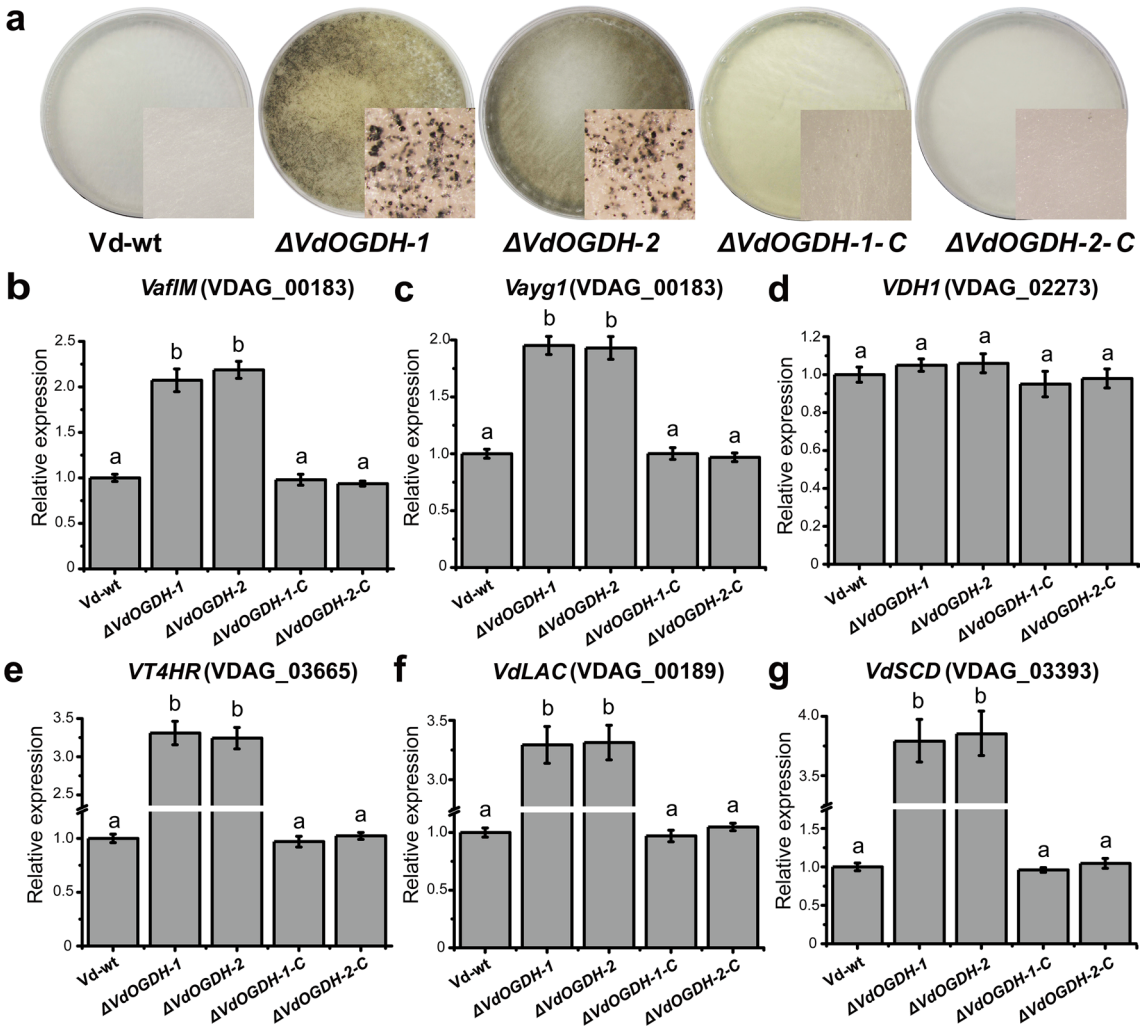

Fig. 5 Microsclerotia production and relative expression of genes related to melanin and microsclerotia production in Vd-wt, *ΔVdOGDH*, and *ΔVdOGDH-C* strains. **a** Colony morphology after 30 days on BMM plates. *ΔVdOGDH* strains produced many more microsclerotia, and colonies thus looked darker, **b**–**g** Mean (±SD) relative gene expression in mycelia after growth in CM for 5 days as determined by qRT-PCR with gene-specific primers. **b** Versicolorin reductase (VDAG_00183, *VaflM*), **c** pigment biosynthesis protein Ayg1 (VDAG_04954, *Vayg1*), **d** class II hydrophobin (VDAG_02273, *VDH1*), **e** tetrahydroxynaphthalene reductase (VDAG_03665, *VT4HR*), **f** laccase (VDAG_00189, *VdLAC*) and **g** scytalone dehydratase (VDAG_03393, *VdSCD*). Internal standard: actin (VDAG_00941). The experiment was done three times. Different letters above the bars indicate a significant difference among strains ($P < 0.05$)

penetrating host plant, adapting to the intracellular environment of the host and enabling pathogenicity in hosts (Luo et al. 2014) and include genes such as transcription activator *Vta2* (Tran et al. 2014), a catalytic subunit of membrane-bound NADPH oxidases gene (*VdNoxB*) and a tetraspanin gene (*VdPls1*) (Zhao et al. 2016), a putative nucleotide-rhamnose synthase/epimerase-reductase gene (*VdNRS/ER*) (Santhanam et al. 2017), a specific secreted protein gene (*VdSCP7*) (Zhang et al. 2017) and defoliating phenotype-related gene (*VdDf7*) (Zhang et al. 2019). Genes contributing to vegetative growth are not completely correlated with virulence; however, genes involved in virulence are more or less correlated with vegetative growth in *V. dahliae* (Luo et al. 2014).

VdOGDH may be classified as a gene related to vegetative growth and indirectly related to virulence in *V. dahliae*. We showed here that it functions in energy metabolism and contributes to multiple virulence-related traits in *V. dahliae*. In the *ΔVdOGDH* mutants, vegetative growth was significantly reduced on different carbon sources, and conidial and hyphal morphology were abnormal, which combined with increased sensitivity to oxidative stress may limit infection and colonization by *ΔVdOGDH* mutants. Furthermore, the reduction in disease severity and fungal biomass in infected cotton plants also suggests that *VdOGDH* contributes to full virulence of *V. dahliae*.

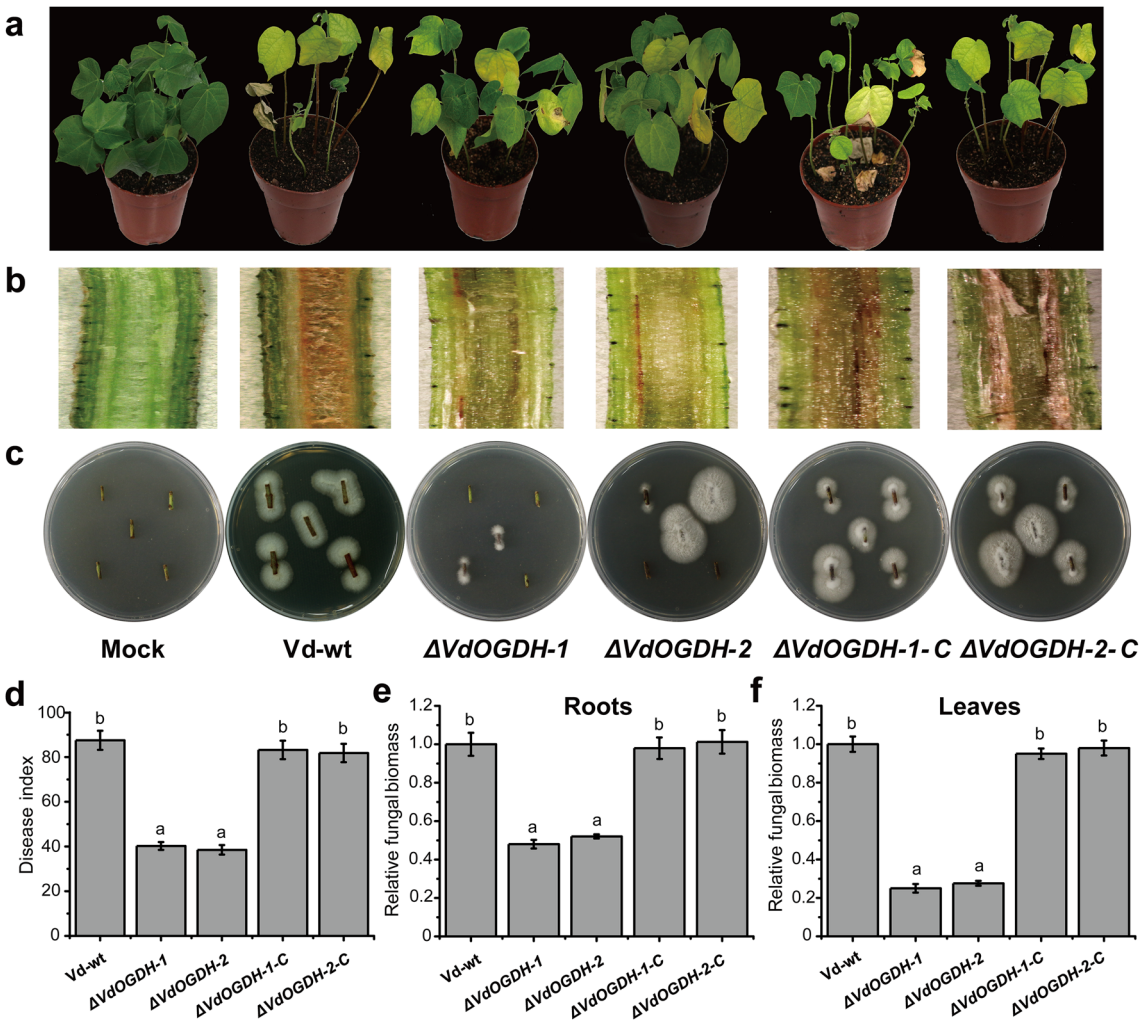

Fig. 6 Pathogenicity tests and fungal biomass in Coker 312 cotton seedlings with 2–3 true leaves. At 30 days post-inoculation with a conidial suspension (10 mL, 10^7 conidia/mL) of Vd-wt, *ΔVdOGDH* or *ΔVdOGDH-C* strains. **a** Disease phenotypes, **b** vascular discoloration of stems tissues of cotton seedlings. **c** Fungal colonies growing from infected cotton stems on PDA. **d** Mean (±SD) disease index. **e**, **f** Mean (±SD) relative fungal biomass in **e** roots and **f** leaves determined by qRT-PCR. Cotton seedlings dipped in sterile water served as controls. The experiments were done three times. Different letters above bars indicate a significant difference among strains ($P < 0.05$)

In summary, *VdOGDH*, which is involved in energy metabolism, regulates carbon utilization, vegetative growth, melanin production, and oxidative stress and is essential for the full virulence of *V. dahliae*.

Acknowledgements This research was supported by a grant from the National Natural Science Foundation of China (31701861 and 31772244), the special fund for agro-scientific research in the public interest (201503109), and the Agricultural Science and Technology Innovation Program of CAAS, and the Fundamental Research Funds for Central Non-profit Scientific Institution (Y2017JC57).

Compliance with ethical standards

Conflict of interest The authors declare that they have no conflict of interest.

Ethical approval This article does not contain any studies with human participants performed by any of the authors.

References

Bai YW, Hu DF, Hu XP et al (2011) Formation conditions for microsclerotia of *Verticillium dahliae*. Mycosystema 30:695–701. https://doi.org/10.13346/j.mycosystema.2011.05.001

Bowyer P, Mueller E, Lucas J (2000) Use of an isocitrate lyase promoter-GFP fusion to monitor carbon metabolism of the plant pathogen *Tapesia yallundae* during infection of wheat. Mol Plant Pathol 1:253–262. https://doi.org/10.1046/j.1364-3703.2000.00030.x

Bunik VI, Fernie AR (2009) Metabolic control exerted by the 2-oxoglutarate dehydrogenase reaction: a cross-kingdom comparison of the crossroad between energy production and nitrogen assimilation. Biochem J 422:405–421. https://doi.org/10.1042/BJ20090722

Butler MJ, Day AW (1998) Fungal melanins: a review. Can J Microbiol 44:1115–1136. https://doi.org/10.1139/w98-119

Cadenas E, Davies KJA (2000) Mitochondrial free radical generation, oxidative stress, and aging. Free Radic Biol Med 39:222–230. https://doi.org/10.1016/S0891-5849(00)00317-8

Chen JY, Liu C, Gui YJ et al (2018a) Comparative genomics reveals cotton-specific virulence factors in flexible genomic regions in *Verticillium dahliae* and evidence of horizontal gene transfer from *Fusarium*. New Phytol 217:756–770. https://doi.org/10.1111/nph.14861

Chen W, Wei L, Zhang Y et al (2018b) Involvement of the two L-lactate dehydrogenase in development and pathogenicity in *Fusarium graminearum*. Curr Genet 65:591–605. https://doi.org/10.1007/s00294-018-0909-6

Divon HH, Fluhr R (2007) Nutrition acquisition strategies during fungal infection of plants. FEMS Microbiol Lett 266:65–74. https://doi.org/10.1111/j.1574-6968.2006.00504.x

Duressa D, Anchieta A, Chen DQ et al (2013) RNA-seq analyses of gene expression in the microsclerotia of *Verticillium dahliae*. BMC Genomics 14:2–18. https://doi.org/10.1186/1471-2164-14-607

Fan R, Klosterman SJ, Wang C et al (2017) *Vayg1* is required for microsclerotium formation and melanin production in *Verticillium dahliae*. Fungal Genet Biol 98:1–11. https://doi.org/10.1016/j.fgb.2016.11.003

Foster AJ, Littlejohn GR, Soanes DM et al (2016) Strategies for nutrient acquisition by *Magnaporthe oryzae* during the infection of rice. In: Unden G, Eckhard T, Anja S (eds) Host-pathogen interaction: microbial metabolism, pathogenicity and antiinfectives. Wiley, Hoboken, pp 93–108

Fradin EF, Thomma BP (2006) Physiology and molecular aspects of *Verticillium* wilt diseases caused by *V. dahliae* and *V. albo-atrum*. Mol Plant Pathol 7:71–86. https://doi.org/10.1111/j.1364-3703.2006.00323.x

Gao F, Zhou BJ, Li GY et al (2010) A glutamic acid-rich protein identified in *Verticillium dahliae* from an insertional mutagenesis affects microsclerotial formation and pathogenicity. PLoS One 5:e15319. https://doi.org/10.1371/journal.pone.0015319

Gibson GE, Blass JP, Beal MF et al (2005) The α-ketoglutarate-dehydrogenase complex. Mol Neurobiol 31:43–64. https://doi.org/10.1385/mn:31:1-3:043

Han Q, Wu F, Wang X et al (2015) The bacterial lipopeptide iturins induce *Verticillium dahliae* cell death by affecting fungal signalling pathways and mediate plant defence responses involved in pathogen-associated molecular pattern-triggered immunity. Environ Microbiol 17:1166–1188. https://doi.org/10.1111/1462-2920.12538

Hao YQ, Lu GQ, Wang LH et al (2018) Overexpression of *AmDUF1517* enhanced tolerance to salinity, drought, and cold stress in transgenic cotton. J Integr Agric 17:2204–2214. https://doi.org/10.1016/s2095-3119(17)61897-5

Hawke MA, Lazarovits G (1994) Production and manipulation of individual microsclerotia of *Verticillium dahliae* for use in studies of survival. Phytopathology 23:582–584. https://doi.org/10.1094/Phyto-84-883

Hu D, Wang C, Tao F et al (2014) Whole genome wide expression profiles on germination of *Verticillium dahliae* microsclerotia. PLoS One 9:e100046. https://doi.org/10.1371/journal.pone.0100046

Jonkers W, Van Kan JAL, Tijm P et al (2011) The *FRP1* F-box gene has different functions in sexuality, pathogenicity and metabolism in three fungal pathogens. Mol Plant Pathol 12:548–563. https://doi.org/10.1111/j.1364-3703.2010.00689.x

Khang CH, Park SY, Lee YH et al (2005) A dual selection based, targeted gene replacement tool for *Magnaporthe grisea* and *Fusarium oxysporum*. Fungal Genet Biol 42:483–492. https://doi.org/10.1016/j.fgb.2005.03.004

Khosravi C, Benocci T, Battaglia E et al (2015) Sugar catabolism in *Aspergillus* and other fungi related to the utilization of plant biomass. Adv Appl Microbiol 90:1–28. https://doi.org/10.1016/bs.aambs.2014.09.005

Klimes A, Dobinson KF (2006) A hydrophobin gene, *VDH1*, is involved in microsclerotial development and spore viability in the plant pathogen *Verticillium dahliae*. Fungal Genet Biol 43:283–294. https://doi.org/10.1016/j.fgb.2005.12.006

Klimes A, Amyotte SG, Grant S et al (2008) Microsclerotia development in *Verticillium dahliae*: regulation and differential expression of the hydrophobin gene *VDH1*. Fungal Genet Biol 45:1525–1532. https://doi.org/10.1016/j.fgb.2008.09.014

Klimes A, Dobinson KF, Thomma BP et al (2015) Genomics spurs rapid advances in our understanding of the biology of vascular wilt pathogens in the genus *Verticillium*. Annu Rev Phytopathol 53:181–198. https://doi.org/10.1146/annurev-phyto-080614-120224

Klosterman SJ, Atallah ZK, Vallad GE et al (2009) Diversity, pathogenicity, and management of *Verticillium* species. Annu Rev Phytopathol 47:39–62. https://doi.org/10.1146/annurev-phyto-080508-081748

Klosterman SJ, Subbarao KV, Kang S et al (2011) Comparative genomics yields insights into niche adaptation of plant vascular wilt pathogens. PLoS Pathog 7:e1002137. https://doi.org/10.1371/journal.ppat.1002137

Kotchoni SO, Gachomo EW (2006) The reactive oxygen species network pathways: an essential prerequisite for perception of pathogen attack and the acquired disease resistance in plants. J Biosci 31:389–404. https://doi.org/10.1007/bf02704112

Livak KJ, Schmittgen TD (2001) Analysis of relative gene expression data using real-time quantitative PCR and the $2^{-\Delta\Delta CT}$ method. Methods 25:402–408. https://doi.org/10.1006/meth.2001.1262

Lorenz MC, Fink GR (2001) The glyoxylate cycle is required for fungal virulence. Nature 412:83–86. https://doi.org/10.1038/35083594

Luo X, Xie C, Dong J et al (2014) Interactions between *Verticillium dahliae* and its host: vegetative growth, pathogenicity, plant immunity. Appl Microbiol Biot 98:6921–6932. https://doi.org/10.1007/s00253-014-5863-8

Luo X, Mao H, Wei Y et al (2016) The fungal-specific transcription factor *Vdpf* influences conidia production, melanized microsclerotia formation and pathogenicity in *Verticillium dahliae*. Mol Plant Pathol 17:1364–1381. https://doi.org/10.1111/mpp.12367

McKinney JD, HzB K, Muñoz-Elías EJ et al (2000) Persistence of *Mycobacterium tuberculosis* in macrophages and mice requires the glyoxylate shunt enzyme isocitrate lyase. Nature 406:735–738. https://doi.org/10.1038/35021074

Pegg GF, Brady BL (2002) *Verticillium* Wilts. CABI Pulishing, NewYork

Qi X, Su X, Guo H et al (2016) VdThit, a thiamine transport protein, is required for pathogenicity of the vascular pathogen *Verticillium dahliae*. Mol Plant Microbe Interact 29:545–559. https://doi.org/10.1094/MPMI-03-16-0057-R

Qi X, Li X, Guo H et al (2018) VdPLP, A patatin-like phospholipase in *Verticillium dahliae*, is involved in cell wall integrity and required for pathogenicity. Genes 9:e162. https://doi.org/10.3390/genes9030162

Rauyaree P, Ospina-Giraldo MD, Kang S et al (2005) Mutations in *VMK1*, a mitogen-activated protein kinase gene, affect microsclerotia formation and pathogenicity in *Verticillium dahliae*. Curr Genet 48:109–116. https://doi.org/10.1007/s00294-005-0586-0

Rehman L, Su X, Guo H et al (2016) Protoplast transformation as a potential platform for exploring gene function in *Verticillium dahliae*. BMC Biotechnol 16:e57. https://doi.org/10.1186/s12896-016-0287-4

Rehman L, Su X, Li X et al (2017) *FreB* is involved in the ferric metabolism and multiple pathogenicity-related traits of *Verticillium dahliae*. Curr Genet 64:645–659. https://doi.org/10.1007/s00294-017-0780-x

Repetto B, Tzagoloff A (1989) Structure and regulation of *KGD1*, the structural gene for yeast alpha-ketoglutarate dehydrogenase. Mol Cell Biol 9:2695–2705. https://doi.org/10.1128/MCB.9.6.2695

Repetto B, Tzagoloff A (1990) Structure and regulation of *KGD2*, the structural gene for yeast dihydrolipoyl transsuccinylase. Mol Cell Biol 10:4221–4232. https://doi.org/10.1128/mcb.10.8.4221

Sandeman RA, Hynes MJ, Fincham JR et al (1991) Molecular organisation of the malate synthase gene of *Aspergillus nidulans* and *Neurospora crassa*. Mol Genet Genomics 228:445–452. https://doi.org/10.1007/bf00260638

Santhanam P, van Esse HP, Albert I et al (2013) Evidence for functional diversification within a fungal NEP1-like protein family. Mol Plant Microbe Interact 26:278–286. https://doi.org/10.1094/MPMI-09-12-0222-R

Santhanam P, Boshoven JC, Salas O et al (2017) Rhamnose synthase activity is required for pathogenicity of the vascular wilt fungus *Verticillium dahliae*. Mol Plant Pathol 18:347–362. https://doi.org/10.1111/mpp.12401

Shi Y, Wang H, Yan Y et al (2018) Glycerol-3-phosphate shuttle is involved in development and virulence in the rice blast fungus *Pyricularia oryzae*. Front Plant Sci 9:e687. https://doi.org/10.3389/fpls.2018.00687

Solomon PS, Tan KC, Oliver RP (2003) The nutrient supply of pathogenic fungi; a fertile field for study. Mol Plant Pathol 4:203–210. https://doi.org/10.1046/j.1364-3703.2003.00161.x

Solomon PS, Lee RC, Wilson TJ et al (2004) Pathogenicity of *Stagonospora nodorum* requires malate synthase. Mol Microbiol 53:1065–1073. https://doi.org/10.1111/j.1365-2958.2004.04178.x

Su X, Rehman L, Guo H et al (2017) The oligosaccharyl transferase subunit *STT3* mediates fungal development and is required for virulence in *Verticillium dahliae*. Curr Genet 64:235–246. https://doi.org/10.1007/s00294-017-0729-0

Tao L, Zhang Y, Fan S et al (2017) Integration of the tricarboxylic acid (TCA) cycle with cAMP signaling and Sfl2 pathways in the regulation of CO_2 sensing and hyphal development in *Candida albicans*. PLoS Genet 13:e1006949. https://doi.org/10.1371/journal.pgen.1006949

Thines E, Weber RW, Talbot NJ (2000) MAP kinase and protein kinase A-dependent mobilization of triacylglycerol and glycogen during appressorium turgor generation by *Magnaporthe grisea*. Plant Cell 12:1703–1718. https://doi.org/10.2307/3871184

Tian H, Zhou L, Guo W et al (2015) Small GTPase Rac1 and its interaction partner Cla4 regulate polarized growth and pathogenicity in *Verticillium dahliae*. Fungal Genet Biol 74:21–31. https://doi.org/10.1016/j.fgb.2014.11.003

Tran VT, Braus-Stromeyer SA, Kusch H et al (2014) *Verticillium* transcription activator of adhesion Vta2 suppresses microsclerotia formation and is required for systemic infection of plant roots. New Phytol 202:565–581. https://doi.org/10.1111/nph.12671

Tzima A, Paplomatas EJ, Rauyaree P et al (2010) Roles of the catalytic subunit of cAMP-dependent protein kinase A in virulence and development of the soilborne plant pathogen *Verticillium dahliae*. Fungal Genet Biol 47:406–415. https://doi.org/10.1016/j.fgb.2010.01.007

Vallad GE, Subbarao KV (2008) Colonization of resistant and susceptible lettuce cultivars by a green fluorescent protein-tagged isolate of *Verticillium dahliae*. Phytopathology 98:871–885. https://doi.org/10.1094/PHYTO-98-8-0871

Voegele RT, Hahn M, Lohaus G et al (2005) Possible roles for mannitol and mannitol dehydrogenase in the biotrophic plant pathogen *Uromyces fabae*. Plant Physiol 137:190–198. https://doi.org/10.1104/pp.104.051839

Voet D, Voet JG, Pratt CW (2016) Fundamentals of biochemistry: life at the molecular level, fifth, ed edn. John Wiley & Sons Inc., Hoboken

Wang ZY, Thornton CR, Kershaw MJ et al (2003) The glyoxylate cycle is required for temporal regulation of virulence by the plant pathogenic fungus *Magnaporthe grisea*. Mol Microbiol 47:1601–1612. https://doi.org/10.1046/j.1365-2958.2003.03412.x

Wang C, Lu G, Hao Y et al (2017) ABP9, a maize bZIP transcription factor, enhances tolerance to salt and drought in transgenic cotton. Planta 246:453–469. https://doi.org/10.1007/s00425-017-2704-x

Xie CJ, Wang CY, Wang XK et al (2013) Proteomics-based analysis reveals that *Verticillium dahliae* toxin induces cell death by modifying the synthesis of host proteins. J Gen Plant Pathol 79:335–345. https://doi.org/10.1007/s10327-013-0467-1

Xiong D, Wang Y, Tang C et al (2015) *VdCrz1* is involved in microsclerotia formation and required for full virulence in *Verticillium dahliae*. Fungal Genet Biol 82:201–212. https://doi.org/10.1016/j.fgb.2015.07.011

Xu M, Gui YJ, Qi WY et al (2013) *Verticillium dahliae* labeled with green fluorescent protein gene. Plant Protect 39:128–133. https://doi.org/10.3969/j.issn.0529-1542.2013.05.018

Yang YL, Liu ZY, Cai L et al (2009) *Colletotrichum anthracnose* of Amaryllidaceae. Fungal Divers 39:123–146. https://doi.org/10.1007/s10327-005-0214-3

Yang X, Ding F, Zhang L et al (2015) The importin alpha subunit PsIMPA1 mediates the oxidative stress response and is required for the pathogenicity of *Phytophthora sojae*. Fungal Genet Biol 82:108–115. https://doi.org/10.1016/j.fgb.2015.04.023

Yun BW, Feechan A, Yin M et al (2011) *S*-nitrosylation of NADPH oxidase regulates cell death in plant immunity. Nature 478:264–268. https://doi.org/10.1038/nature10427

Zhang WW, Jian GL, Jiang TF et al (2012) Cotton gene expression profiles in resistant *Gossypium hirsutum* cv. Zhongzhimian KV1 responding to *Verticillium dahliae* strain V991 infection. Mol Biol Rep 39:9765–9774. https://doi.org/10.1007/s11033-012-1842-2

Zhang L, Ni H, Du X et al (2017) The *Verticillium*-specific protein VdSCP7 localizes to the plant nucleus and modulates immunity to fungal infections. New Phytol 215:368–381. https://doi.org/10.1111/nph.14537

Zhang DD, Wang J, Wang D et al (2019) Population genomics demystifies the defoliation phenotype in the plant pathogen *Verticillium dahliae*. New Phytol. https://doi.org/10.1111/nph.15672

Zhao YL, Zhou TT, Guo HS (2016) Hyphopodium-specific VdNoxB/VdPls1-dependent ROS-Ca^{2+} signaling is required for plant infection by *Verticillium dahliae*. PLoS Pathog 12:e1005793. https://doi.org/10.1371/journal.ppat.1005793

Zhao Y-L, Zhang T, Guo H-S (2017) Penetration assays, fungal recovery and pathogenicity assays for *Verticillium dahliae*. Bio-Protocol 7:1–8. https://doi.org/10.21769/BioProtoc.2133

Zhou BJ, Jia PS, Gao F et al (2012) Molecular characterization and functional analysis of a necrosis- and ethylene-inducing, protein-encoding gene family from *Verticillium dahliae*. Mol Plant Microbe Interact 25:964–975. https://doi.org/10.1094/MPMI-12-11-0319

Zhu H-Q, Feng Z-L, Li Z-F et al (2013) Characterization of two fungal isolates from cotton and evaluation of their potential for biocontrol of *Verticillium* wilt of cotton. J Phytopathol 161:70–77. https://doi.org/10.1111/jph.12027